American Journal of Pathology, Vol. 154, No. 4, April 1999

Animal Model

Transgenic Mouse Model of AA Amyloidosis

Alan Solomon,* Deborah T. Weiss,* Maria Schell,* Rudi Hrncic,* Charles L. Murphy,* Jonathan Wall,* M. Donald McGavin,† Hong Jun Pan,‡ George W. Kabalka,‡ and Michael J. Paulus§

From the Department of Medicine, the Human Immunology and Cancer Program, and the Department of Radiology,‡ University of Tennessee Medical Center/Graduate School of Medicine, Knoxville, Tennessee; the Department of Pathology,† University of Tennessee College of Veterinary Medicine, Knoxville, Tennessee; and the Instrumentation and Controls Division,§ Oak Ridge National Laboratory, Oak Ridge, Tennessee*

AA amyloidosis can be induced in mice experimentally through injection of certain chemical or biological compounds. However, the usefulness of this approach is limited by its dependence on exogenous inflammatory agents that stimulate cytokines to increase the synthesis of precursor serum amyloid A (SAA) protein and the transitory nature of the pathological fibrillar deposits. We now report that transgenic mice carrying the human interleukin 6 gene under the control of the metallothionein-I promoter had markedly increased concentrations of SAA and developed amyloid in the spleen, liver, and kidneys by 3 months of age. At the time of death about 6 months later, organs obtained from these animals had extensive amyloid deposits. This disease process was apparent radiographically using small-animal computer axial tomography and magnetic resonance imaging equipment. The AA nature of the amyloid was evidenced immunohistochemically and was unequivocally established by sequence analysis of protein extracted from the fibrils. The availability of this unique *in vivo* experimental model of AA amyloidosis provides the means to assess the therapeutic efficacy of agents designed to reduce or prevent the fibrillar deposits found in AA and other types of amyloid-associated disease. *(Am J Pathol 1999, 154:1267–1272)*

Elucidation of the pathogenesis, treatment, and prevention of diseases associated with amyloid fibril deposition has been hampered by the lack of suitable *in vivo* experimental models that can reproduce the salient features of amyloidosis. Historically, one approach that has been extensively used to study AA amyloidosis, a particular form of this disorder, involves injecting mice with one of a variety of chemical or biological compounds including casein, silver nitrate, and lipopolysaccharide.[1,2] These agents stimulate the production of cytokines, eg, tumor necrosis factor and interleukins 1 and 6 (IL-1 and IL-6), that mediate the inflammatory response by increasing the hepatic synthesis of serum amyloid A protein (SAA).[3] This molecule, in turn, serves as the precursor of the polypeptide that is deposited in the spleen, liver, and kidneys of affected animals as Congophilic, green birefringent fibrils, ie, AA amyloid.[4–7] Because cessation of the exogenous inflammatory stimulus results in resorption of the amyloid deposits,[2] the usefulness of this model is limited by the need for repeated injections and the transitory nature of the induced pathology.

Through transgenic technology, it is now possible to study the pathological effects of continuous expression of cytokines and other biological factors. Because IL-6 plays a seminal role in hematopoiesis and the inflammatory-mediated response,[8–12] transgenic mice have been generated that express the murine (mIL-6)[13,14] or human (hIL-6)[15,16] form of this molecule. Animals carrying the hIL-6 gene under the control of either the human Eμ enhancer[15] or the mouse metallothionein-I (MT-I) promoter[16] predominantly express IL-6 in B cells or liver, respectively. The Eμ/hIL-6 transgenic mice are typified by an extensive polyclonal plasma cell proliferation within lymph nodes and spleen, as well as a mesangioproliferative glomerulonephritis.[15] The MT-I/hIL-6 animals have a sustained increase in liver-derived acute phase proteins and an IgG plasmacytosis within lymphoid tissue; in addition, these mice manifest renal pathology resembling that seen in patients with myeloma (cast) nephropathy.[16] In studies of these animals we have also observed that, in contrast to the Eμ/hIL-6 transgenics, the MT-I/hIL-6 mice develop by 3 months of age amyloid deposition in spleen, liver, and renal glomeruli, as evidenced by polarizing and electron microscopy. At the time of death 5 to 7 months

Supported in part by U.S. Public Health research grant CA 10056 from the National Cancer Institute and National Science Foundation grant BIR-94 08252. A. S. is an American Cancer Society Clinical Research Professor.

Accepted for publication January 21, 1999.

Address reprint requests to Dr. Alan Solomon, University of Tennessee Medical Center, 1924 Alcoa Highway, Knoxville, TN 37920. E-mail: asolomon@MC.UTMCK.edu.

later, the pathological process has progressed as evidenced by marked hepatosplenomegaly associated with prominent areas of Congophilic, green birefringent material that is fibrillar when viewed by electron microscopy. We have shown immunohistochemically that the amyloid deposits are AA-related. Further, sequence analyses of molecules extracted from the amyloid confirmed they were products of the mouse SAA_2 gene.[17] The MT-I/hIL-6 transgenic mice provide a new experimental *in vivo* model in which to study factors involved in the pathogenesis of amyloid deposition and to test potential therapeutic agents that can limit or prevent fibril formation.

Materials and Methods

Generation of Transgenic Animals

Transgenic mice carrying the hIL-6 cDNA under the control of the mouse MT-I promoter and Eμ enhancer were furnished by Dr. Gennaro Ciliberto and Dr. Michael Potter, respectively. The MT-I/hIL-6 mice were generated as previously described.[16] Briefly, a gel-purified 4.25 Kb *Pvu*II-*Pvu*II DNA fragment containing the hIL-6 cDNA was cloned downstream of the MT-I promoter and microinjected into the pronuclei of fertilized eggs of a cross-F1 (C57BL/6JXDBAII) mouse.

Southern Blot Analysis

Tail-derived DNA was isolated and digested with *Pvu*II (New England Biolabs, Beverly, MA). Southern blots were performed[18] using a purified, labeled IL-6-specific DNA fragment (provided by Dr. Robert Hall) as a probe. The blots were hybridized and washed under stringent conditions (65°C, 0.1× SSC) and exposed to X-ray film overnight.

Polymerase Chain Reaction

Mice were genotyped for the presence of the transgene through analyses of genomic DNA. IL-6-specific primers were designed that amplified a 450-bp fragment containing the internal segment of the hIL-6 gene. The sequence of the upstream primer (IL-6For) was 5′ ACC TCT TCA GAA CGA ATT GAC AAA 3′ whereas that of the downstream primer (IL-6Rev) was 5′ AGC TGC GCA GAA TGA GAT GAG TTG T 3′. One microgram of genomic mouse DNA isolated from tail clippings served as the template for 30 cycles of polymerase chain reaction (PCR) amplification using a commercial kit (Applied Biosystems-Perkin Elmer, Foster City, CA) and 0.5 μmol/L of each primer (final concentration) in a total reaction volume of 100 μl. The time and temperature for each cycle were, for denaturation, 1 minute at 94°C; for annealing, 1 minute at 60°C; and for extension, 1.5 minutes at 72°C. For the first and last cycles the reaction times were extended to 3 and 7 minutes, respectively.

Histopathology

For light microscopy, 4- to 6-μm tissue sections were cut and stained with hematoxylin and eosin. To detect amyloid, the sections were also treated with a freshly prepared alkaline Congo red solution and viewed under polarized light using a filter polarizer (Leitz, Rockleigh, NJ) with a gypsum plate and a filter analyzer. For electron microscopy, sections embedded in Epon (Electron Microscopy Sciences, Fort Washington, PA) were examined with a Zeiss 9S transmission electron microscope and photographed.

Immunohistochemistry

Six-μm paraffin-embedded tissue sections were cut on a microtome, mounted on poly-L-lysine-coated slides, dried overnight at room temperature, and deparaffinized. Immunostaining was performed using the avidin-biotin complex (ABC) technique (Vector Laboratories, Burlingame, CA) as described previously.[19] The primary antibodies included rabbit anti-mouse SAA(provided by Drs. M. Kindy and F. DeBeer); an affinity-purified goat anti-mouse IgG (H+L) horseradish peroxidase conjugate (BioRad Laboratories, Richmond, CA); and sheep anti-mouse serum AP (provided by Dr. M. B. Pepys). A biotinylated sheep anti-rabbit globulin antiserum was used as the secondary antibody.

Protein Assays

Serum concentrations of mouse SAA were measured in an enzyme-linked immunosorbent assay according to directions supplied by the manufacturer (Biosource, Camarillo, CA). Briefly, sera were collected from transgenic and control mice and analyzed using a commercial cytoscreen immunoassay kit and a specific rat anti-human SAA mAb. A standard curve was made from known amounts of mouse SAA protein and absorbance was measured at 405 nm with a model 450 BioRad plate reader. Serum IL-6 activity was assayed using the 7TD1 proliferation assay[11] and hIL-6 recombinant protein (Gibco-BRL, Bethesda, MD). A standard curve was prepared from 1, 10, 100, and 1000 pg/ml of hIL-6 in a final sample volume of 100 μl. One unit of IL-6 corresponded to 1 and 7 pg of mouse and human IL-6, respectively.

Amyloid Extraction and Purification

The methods used to extract amyloid from tissue were as described by Pras et al.[20] Mouse tissue was homogenized with cold saline in an ice bath using an Omni-Mixer (Omni International, Waterbury, CT). The extract was centrifuged at 10,000 rpm for 30 minutes at 4°C and the pellet re-extracted twice more with cold saline, once with 0.1 mol/L sodium citrate Tris-buffered saline, pH 8.0, and then with saline until the A_{280} of the supernatant was <0.10. The resultant 10,000-rpm pellet was homogenized with cold distilled water and the extract centrifuged

at 35,000 rpm for 3 hours at 4°C. The pellet obtained from the water extract was then lyophilized.

One milligram of extracted amyloid protein was dissolved in 6 mol/L guanidine HCl, 0.25 mol/L Tris-HCl buffer, pH 8.0, reduced and alkylated,[21] and purified using an ABI Model 151 HPLC apparatus and a Brownlee Aquapore 300A C8 reversed-phase 210 × 4.6 mm column (Perkin-Elmer, Norwalk, CT) with a 0.1% TFA/70% acetonitrile/water (v/v) linear gradient at a flow rate of 1 ml/minute.[21] Protein was detected by absorbance at 220 nm and fractions were collected manually.

Sequence Analysis

Automated sequence analyses by Edman degradation were performed using an ABI model 477A pulsed liquid sequenator; the resulting phenylthiohydantoin amino acids were identified with an on-line ABI model 120A phenylthiohydantoin amino acid analyzer.

Mass Spectroscopy

Mass spectroscopy was performed at the University of Tennessee Mass Spectroscopy Center, which houses an electrospray ionization triple quadrapole instrument (Quattro II, Micromass, Manchester, UK). The multiple charged peaks were resolved to their true molecular mass (*M*r) by the MaxEnt program contained in the Max Lynx software package, as supplied by the manufacturer.

Magnetic Resonance Imaging

Multiple spin echo images were obtained on a Bruker AMX-400 nuclear magnetic resonance spectrometer (9.3 Telsa, 89-mm bore). A Bruker imaging probe with a 25-mm coil was used with repetition time of 2 seconds, an echo time of 8.3 milliseconds, and a 2.0-mm slice thickness. Images represent the average of two acquisitions.

Computer Axial Tomography

High resolution X-ray computed tomography images were acquired using the Oak Ridge National Laboratory MicroCAT apparatus designed specifically for small laboratory animals (M. J. Paulus, manuscript in preparation). The MicroCAT uses a 1024 × 1024 element CCD-based detector with an intrinsic spatial resolution of ~50 μm and a data acquisition rate of ~30 projections per minute. Typical data sets consist of 180 projections for screening studies and 500 projections for high-resolution studies. Two- and three-dimensional reconstructed images are obtained using a cone beam-filtered back-projection algorithm.

Results

Molecular Characterization of Transgenic Mice

Two MT-I/hIL-6 transgenic female mice (designated nos. 3 and 4) and a wild-type male (no. 5), furnished by Dr. Gennaro Ciliberto, were used to establish a breeding colony at the University of Tennessee Medical Center. The presence of the hIL-6 gene in the female carriers was verified by Southern blot analysis and PCR amplification of DNA obtained from tail clippings using a probe and primers specific for IL-6. The first mating of mice 3 and 5 yielded five offspring, two of which carried the hIL-6 transgene as evidenced by the presence in Southern blots of the characteristic 4.25-kb *Pvu*II band.[16]

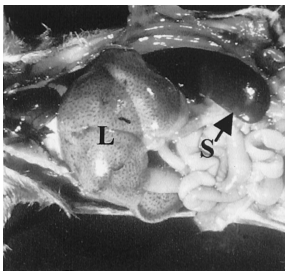

Figure 1. Necroscopic examination of an MT-1/hIL-6 transgenic mouse. The markedly enlarged liver (L) and spleen (S) are indicated.

Clinical and Laboratory Features

The two hIL-6 transgenic mice appeared healthy until ~8 to 9 months of age, when they assumed a hunched appearance and became increasingly moribund. Their serum IL-6 and SAA concentrations were markedly elevated (46 units/μl and 1067 μg/ml, respectively) compared to an age-matched wild-type control mouse in which these components were virtually undetectable. Additionally, the transgenic animals had a profound polyclonal hypergammaglobulinemia and renal failure, as evidenced by proteinuria and an increased blood urea nitrogen of 79 mg/dl. X-ray studies revealed hepatosplenomegaly and osteopenia.

Pathological Features

The salient pathology found in mouse no. 4 (euthanized at 8 months of age) was confined to the spleen, liver, kidney, and bones. The spleen was greatly enlarged and measured 42 mm long by 10 mm wide (Figure 1). The cut surface had a white, mottled appearance. By light microscopy, a pronounced plasma cell infiltrate and extramedullary hematopoiesis were seen. The liver was also enlarged (Figure 1) and its visceral surface was covered by an exaggerated reticular pattern; portal areas appeared as red, triangular foci in the pale surface. The adjacent hepatocytes were atrophic and the lumens of the sinusoids were narrowed. A prominent perivenular granulocytic infiltration was noted. The kidneys, although normal in size, were pale in appearance. Histologically, the renal glomeruli were atrophic and the tubules dilated and filled with proteinaceous casts. A thick perivascular cuff of plasmacytoid cells surrounded renal blood vessel walls. The bones were fragile with marked osteopenia characterized by thin cortices and loss of cancellous bone. Granulocytic and megakaryocytic hyperplasia and

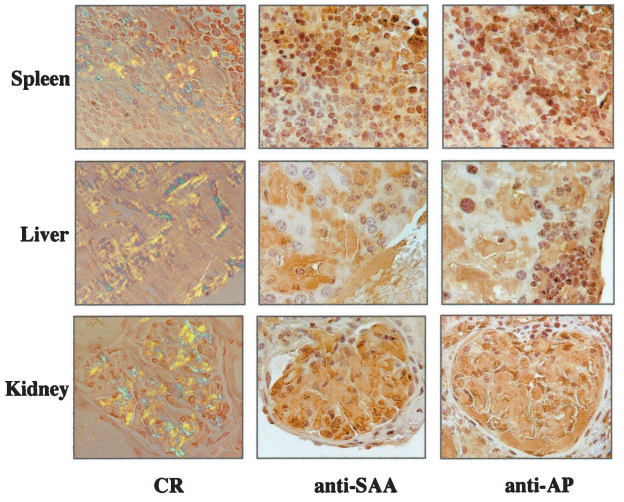

Figure 2. Histochemical and immunohistochemical analyses of spleen, liver, and kidney obtained from an MT-1/hIL-6 transgenic mouse. Left panels: Polarizing microscopy of Congo red (CR)-stained tissue sections. Original magnification, ×400. Middle and right panels: Immunoperoxidase staining with anti-SAA and anti-AP antibodies, respectively. Original magnification, ×400.

scattered foci of plasmacytoid cells were present in the bone marrow and lymph nodes. Congo red staining of tissues (Figure 2) revealed under polarizing microscopy that the mottled areas in the spleen contained green birefringent perifollicular deposits. The spaces of Disse within the liver were widely distended by a Congophilic hyaline substance that exhibited spotty green birefringence and occupied ~50 to 80% of the section. Additionally, green birefringent Congophilic deposits were noted in most glomeruli and throughout the renal medulla. In contrast, the tubular casts were Congo red-negative. Sections of the spleen, liver, and kidney treated with sulfated Alcian blue revealed that the Congophilic areas were also stained by the this reagent.

Electron Microscopy

Areas corresponding to Congophilic, green birefringent material seen in the hepatic parenchyma were found by electron microscopy to contain unbranched fibrils 6–10 nm in diameter (Figure 3). Similar material was also present in the spleen and kidneys (not shown).

Immunohistochemistry

Serial sections of spleen, liver, and kidney from mouse no. 4 were examined using a polyclonal anti-mouse SAA antiserum that had been shown by Drs. F. DeBeer and M. Kindy to recognize murine AA deposits (personal communication). Immunohistochemical analyses revealed that the Congophilic material present in the splenic and hepatic parenchyma and renal glomeruli represented AA protein. When tested against an antibody specific for the mouse amyloid-associated P component (AP), this molecule was also detected in the pathological deposits (Figure 2). Additionally, AA protein was found in the non-Congophilic renal tubular casts, as was mouse IgG and AP (not illustrated).

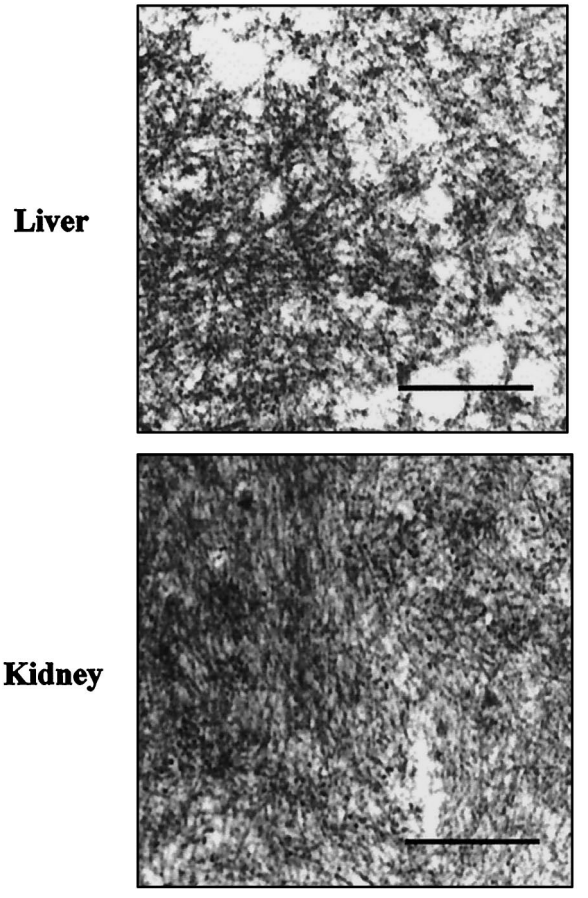

Figure 3. Electronphotomicrographs of fibrils extracted from the liver and kidney of an MT-1/hIL-6 transgenic mouse. Original magnification, ×60,000; scale bar, 325 nm.

Chemical Analyses

Approximately 60 mg of water-soluble protein was extracted from 217 mg (dry weight) of hepatic tissue and purified by high performance liquid chromatography (HPLC). The protein contained in the major HPLC peak consisted of a single species, as evidenced by sodium

```
                    10        20        30        40        50
AA    GFFSFIGEAFQGAGDMWRAYTDMKEAGWKDGDKYFHARGNYDAAQRGPGGVWAAEKIS

MT-I/hIL6  ----------------------------------------------------
```

Figure 4. Comparison of the amino acid sequences of the first 58 residues of mouse AA amyloid *versus* those of protein extracted from the liver of an MT-1/hIL-6 transgenic mouse.

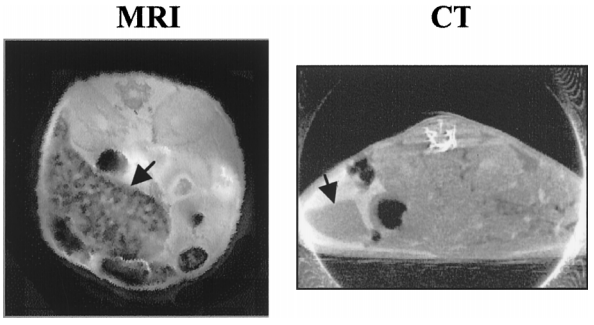

Figure 5. Radiographic imaging of MT-1/hIL-6 transgenic mice. Left: MRI scan, T-1 weighted image, 10-month-old mouse. Right: CT scan, negative contrast, 8-month-old mouse.

dodecyl sulfate-polyacrylamide gel electrophoresis. Direct (automated) analysis of this component yielded 58 amino acid residues that were identical in sequence to the amino-terminal portion of the murine SAA_2 protein (Figure 4). Similar results were obtained when amyloid protein extracted from the spleen was purified by HPLC and sequenced; additionally, ~50% of this material consisted of murine histone H2b-F. By mass spectroscopy, the predominant *Mr* of the purified hepatic amyloid was 8636.4 d, a value virtually identical to that calculated from the amino acid composition of the first 77 amino acid residues of mouse SAA_2.[17] Trace amounts of molecules having *Mr*s of 8434.1, 8565.3, and 8751.4 d were also detected which corresponded to the first 75, 76, and 78 residues, respectively, of this protein.

Radiographic Imaging

The enlarged spleen noted in the MT-I/hIL-6 mouse was especially evident in magnetic resonance imaging (MRI) and computed tomography (CT) scans using equipment designed for small animal imaging (Figure 5). In particular, the mottled areas that contained the amyloid deposits were visualized by MRI. In age-matched control mice the spleen was not visible by these techniques (not illustrated).

Discussion

We have demonstrated that transgenic mice expressing hIL-6 under control of the mouse MT-I promoter developed within the spleen, liver, and kidneys extensive pathological deposits that had the characteristic tinctorial and ultrastructural features of amyloid; namely, they were Congophilic and exhibited green birefringence when examined under polarized light and, by electron microscopy, were fibrillar in nature. Immunohistochemical studies revealed that this material reacted with a specific anti-mouse SAA antiserum. Amino acid sequence analysis of HPLC-purified fibrillar protein extracted from the liver and spleen confirmed the murine AA nature of the amyloid and that it was derived from the amyloidogenic SAA_2 isoform.[17] The *Mr* of the predominant component extracted was ~8600 d and was comparable to that of human and other experimental forms of AA amyloidosis.[2] The presence of other molecules associated with amyloid deposition, eg, AP component and highly sulfated glycosoaminoglycans,[3] was also evidenced. Additionally, histones, which have been found in association with AA amyloid,[22–24] were detected in splenic extracts. Thus, the anatomical location and molecular features of the amyloid deposits found in the MT-I/hIL6 transgenic mice were identical to those typically occurring in experimental models in which AA amyloidosis is induced by inflammatory stimuli.[1–3]

Amyloid deposition in the MT-I/hIL-6 transgenic mice was age-dependent. The pathological deposits were first evident at 3 months of age and increased over the next 6 months as the animals became obviously ill. The progressive nature of the deposition, particularly within the spleen, was readily ascertained by serial MRI examinations using small animal high-resolution radiographic techniques. Notably, this technology (as well as that using radiolabeled P component[25]) will make it possible to monitor noninvasively the effects of therapeutic agents designed to prevent or reverse amyloid formation.

We attribute the development of AA amyloid in the MT-I/hIL-6 transgenic mice to stimulation by IL-6 of liver-derived acute phase reactants that include the AA amyloid precursor protein SAA.[3,9–11] Although MT-I is an inducible promoter,[26] the sustained high serum concentrations of hIL-6 in our animals indicated that this transgene product was constitutively expressed. Mice carrying the hIL-6 gene under control of the Eμ enhancer originally were C57BL/6J, then converted to a BALB/c background (strains of mice that have the amyloidogenic isoform of SAA[3,16,17] and in which amyloid can be readily induced experimentally).[27] Despite the fact that they also had increased SAA levels that were, in fact, comparable to the MT-I/hIL-6 animals, only rarely were amyloid deposits noted in their renal blood vessel walls and intestinal mucosa. Whether the failure of the Eμ/hIL-6 transgenic mice to develop extensive AA amyloid can be ascribed to their major site of cytokine expression (ie, lymph nodes *versus* liver) or to other factors is as yet unknown.

Originally, mice carrying the MT-I/hIL-6 gene died at age 3–4 months due to rapid renal failure that initially included membranous glomerulonephritis followed by focal glomerulosclerosis and, eventually, extensive tubular damage associated with cast formation.[16] However, over time the renal disease occurring in successive generations has become less aggressive and mice currently survive up to ~1 year (G. Ciliberto, personal communication). Notably, in addition to the renal tubular casts, plasma cell infiltrates in spleen and lymph nodes, and manifestations of myelocytic and megakaryocytic hyperplasia, mice now have AA-related amyloid deposits in the spleen, liver, and kidneys. We have found that amyloid deposition can be detected as early as ~3 months of age, progresses over time, and, as is the case with hamsters that develop AA amyloid as a consequence of aging,[28] is more pronounced in females for unknown reasons. Further, mice carrying the hIL6 gene are heterozygotes and attempts to create a homozygote have been unsuccessful, presumably due to prenatal lethality. Studies are in progress to determine whether the initial

onset or extent of amyloid deposition can be accelerated by increasing hIL-6 expression. Such experiments involve stimulating the heavy metal-inducible MT-I promoter[26] by addition of zinc sulfate to the animal's drinking water.

Heretofore, the induction of AA amyloid in mice has been dependent on enhancement of SAA synthesis by exogenous agents including casein, silver nitrate, and lipopolysaccharide.[1–3] In this model, amyloid formation typically occurs 14–21 days postinjection or, at shorter intervals, by coadministration of amyloid enhancing factor.[29] However, without continued stimulation, the amyloid deposits resolve in this induced form of AA.[2] Due to the transient nature and variable extent of amyloid deposition, the usefulness of this and other types of murine AA experimental models is limited. In contrast, the MT-I/hIL-6 transgenic mouse provides a unique *in vivo* system in which to study the pathogenesis of AA amyloid. The spontaneous development of amyloidosis in such animals is not dependent on injection of chemical or biological agents. Further, disease progression, as evidenced by the mottled splenic and hepatic deposits in the enlarged organs, can be readily visualized using noninvasive imaging technology. Thus, these genetically engineered animals are especially valuable in investigations of the therapeutic efficacy of compounds designed to inhibit fibril formation or effect resolution of amyloid deposits. The information gleaned from such studies may have applicability in the prevention and treatment of other types of disorders associated with pathological amyloid deposition such as is found in patients with AL or transthyretin-associated amyloidosis, as well as Alzheimer's disease.

Acknowledgments

Transgenic mice carrying the hIL-6 gene under the control of the MT-I promoter and Eμ enhancer were provided to us by Dr. Gennaro Ciliberto and Dr. Michael Potter, respectively. We thank Dr. Mark Kindy, Dr. Fred DeBeer, Dr. M. B. Pepys, and Dr. Robert Hall for furnishing the reagents specified in the text; Dr. Dorcas Schaefer, Dr. Edward Buonocore, Dr. Robert Kisilevsky, Mr. Bret Brunson, and Mr. Al Tuinmann for assistance in the experimental aspects of this study; and Ms. Valerie Brestel for manuscript preparation.

References

1. Skinner M, Shirahama T, Benson MD, Cohen AS: Murine amyloid protein AA in casein induced experimental amyloidosis. Lab Invest 1997, 36:420–427
2. Kisilevsky R, Young ID: Pathogenesis of amyloidosis. Bailliere's Clinical Rheumatology: Reactive Amyloidosis and the Acute-Phase Response. Vol 8, no 3. Edited by G Husby. London, Bailliere Tindall, 1994, pp 613–626
3. Sipe JD: Amyloidosis. Crit Rev Clin Lab Sci 1994, 31:325–354
4. Husebekk A, Skogen B, Husby G, Marhaug G: Transformation of amyloid precursor SAA to protein AA and incorporation into amyloid fibrils in vivo. Scand J Immunol 1985, 21:282–287
5. Tape C, Tan R, Nesheim M, Kisilevsky R: Direct evidence for circulating apo-SAA as the precursor of tissue AA amyloid deposits. Scand J Immunol 1988, 28:317–324
6. Sipe JD: Amyloidosis. Annu Rev Biochem 1992, 61:947–975
7. Husby G, Marhaug G, Dowton B, Sletten K, Sipe JD: Serum amyloid A (SAA): biochemistry, genetics and the pathogenesis of AA amylodosis. Amyloid Int J Exp Clin Invest 1994, 1:119–137
8. Kishimoto T, Hirano T: Molecular regulation of β lymphocyte response. Annu Rev Immunol 1988, 6:485–512
9. Le J, Vilcek J: Interleukin 6: A multifunctional cytokine regulating immune reactions and the acute phase protein response. Lab Invest 1989, 61:588–602
10. Hirano T, Akira S, Taga T, Kishimoto T: Biological and clinical aspects of interleukin 6. Immunol Today 1990, 11:443–449
11. Van Snick J: Interleukin 6: an overview. Annu Rev Immunol 1990, 8:253–257
12. Fattori E, Cappelletti M, Costa P, Sellitto C, Cantoni L, Carelli M, Faggioni R, Fontuzza G, Ghezzi P, Poli V: Defective inflammatory response in interleukin 6-deficient mice. J Exp Med 1994, 180:1243–1250
13. Brandt SJ, Bodine, DM, Dunbar CE, Nienhuis AW: Dysregulated interleukin 6 expression produces a syndrome resembling Castleman's disease in mice. J Clin Invest 1990, 86:592–599
14. Woodroofe C, Müller W, Rüther U: Long-term consequences of interleukin-6 overexpression in transgenic mice. DNA Cell Biol 1992, 11:587–592
15. Suematsu S, Matsuda T, Aozasa K, Akira S, Nakano N, Ohno S, Miyazaki J, Yamamura K, Hirano T, Kishimoto T: IgG1 plasmacytosis in interleukin 6 transgenic mice. Proc Natl Acad Sci USA 1989, 86:7547–7551
16. Fattori E, Della-Rocca C, Costa P, Giorgio M, Dente B, Pozzi L, Ciliberto G: Development of progressive kidney damage and myeloma kidney in interleukin-6 transgenic mice. Blood 1994, 83:2570–2579
17. Meek RL, Hoffman JS, Benditt EP: Amyloidogenesis: one serum amyloid A isotype is selectively removed from circulation. J Exp Med 1986, 163:499–510
18. Sim GK, Kafatos FC, Jones CW, Koehler MD, Efstratiadis A, Maniatis T: Use of a cDNA library for studies on evolution and developmental expression of the chorion multigene families. Cell 1979, 18:1303–1316
19. Solomon A, Weiss DT, Macy SD, Antonucci RA: Immunocytochemical detection of kappa and lambda light chain V region subgroups in human B-cell malignancies. Am J Pathol 1990, 137:855–862
20. Pras M, Shubert M, Zucker-Franklin D, Rimon A, Franklin EC: The characterization of soluble amyloid prepared in water. J Clin Invest 1968, 47:924–933
21. Eulitz M, Weiss DT, Solomon A: Immunoglobulin heavy-chain-associated amyloidosis. Proc Natl Acad Sci USA 1996, 87:6542–6546
22. Foyn Bruun C, Rygg M, Nordstoga K, Sletten K, Marhaug G: Serum amyloid A protein in mink during endotoxin induced inflammation and amyloidogenesis. Scand J Immunol 1994, 40:337–344
23. Prelli F, Pras M, Shtrasburg S, Frangione B: Characterization of high molecular weight amyloid A proteins. Scand J Immunol 1991, 33:783–7866
24. Nordstoga K, Zhou ZY, Husby G: Bovine glomerular amyloidosis: morphological studies. Zentralbl Veterinarmed A 1994, 41:741–747
25. Gillmore JD, Hawkins PN, Pepys MB: Amyloidosis: a review of recent diagnostic and therapeutic developments. Brit J Haematol 1997, 99:245–256
26. Palmiter RD, Brinster RL: Germ-line transformation of mice. Annu Rev Genet 1986, 20:465–499
27. Suematsu S, Matsusaka T, Matsuda T, Ohno S, Miyazaki J, Yamamura K, Hirano T, and Kishimoto T: Generation of plasmacytomas with the chromosomal translocation t(12;15) in interleukin 6 transgenic mice. Proc Natl Acad Sci USA 1991, 89:232–235
28. Coe JE, Ross MJ: Amyloidosis and female protein in the Syrian hamster: concurrent regulation by sex hormones. J Exp Med 1990, 171:1257–1267
29. Axelrad MA, Kisilevsky R, Willmer J, Chen SJ, Skinner M: Further characterizations of amyloid-enhancing factor. Lab Invest 1982, 47: 139–146